Bufalin suppresses tumour microenvironment-mediated angiogenesis by inhibiting the STAT3 signaling pathway

Ke Xu (cola519@163.com)
Shanghai University https://orcid.org/0000-0002-3942-2767
Kai Fang
East China University of Science and Technology
Yueping Zhan
Shanghai PuTuo District Center Hospital
Yuqian Wang
Shanghai PuTuo District Center Hospital
Chengqi Wu
East China University of Science and Technology
Ruiqiu Zhu
Shanghai PuTuo District Center Hospital
Min Sun
Shanghai PuTuo District Center Hospital
Yanyan Qiu
Shanghai PuTuo District Center Hospital
Zeting Yuan
Shanghai PuTuo District Center Hospital
Xin Liang
East China University of Science and Technology
Peihao Yin
Shanghai PuTuo District Center Hospital

Research

Keywords: angiogenesis, bufalin, colorectal cancer, STAT3, tumor microenvironment

Posted Date: February 23rd, 2021

DOI: https://doi.org/10.21203/rs.3.rs-222601/v1

Abstract

Background

Anti-angiogenesis therapy has increasingly become an important strategy for the treatment of colorectal cancer. Recent studies have shown that tumor microenvironment (TME) promotes tumour angiogenesis. Bufalin is an active compound whose anti-tumor efficacy has been proven by previous studies. However, there are very few studies on the anti-angiogenic effects of bufalin.

Methods

Herein, human umbilical vein endothelial cells (HUVEC) tube formation, migration and adhesion test were used to assess angiogenesis in vitro. Western blot and quantitative PCR were used to detect relevant protein levels and the expressions of mRNAs. Subcutaneous xenograft tumor model and hepatic metastasis model in mice were established to investigate the influence of bufalin on angiogenesis-mediated by TME in vivo.

Results

We found that the angiogenesis mediated by tumor microenvironment cells was significantly inhibited in the present of bufalin. The results demonstrated that the pro-angiogenic gene in HUVEC such as VEGF, PDGFA, E-selectin and P-selectin were downregulated by bufalin, and the downregulation was regulated by inhibiting the STAT3 pathway. Overexpression STAT3 could reverse the inhibitory effect of bufalin on angiogenesis. What is more, few reduction of angiogenesis when bufalin directly acted on tumor microenvironment cells.

Conclusion

Our findings demonstrate that bufalin suppresses tumour microenvironment-mediated angiogenesis by inhibiting the STAT3 signaling pathway of vascular endothelial cells, which reveals that bufalin may be used as a new anti-angiogenic adjuvant therapy medicine in the treatment of colorectal cancer.

Background

Colorectal cancer (CRC) is the third most common cancer worldwide, with a mortality rate of 9% of all cancer-related deaths(1), and the incidence is increasing. It is now widely accepted that angiogenesis plays a key role in tumour development, progression and metastasis. Excessive abnormal angiogenesis is a hallmark of solid tumours(2). The concept of anti-angiogenic therapy arose from the seminal observations of Judah Folkman and colleagues. It has been reported that anti-angiogenic therapy can

effectively improve the survival rate of CRC patients, which manifests that inhibiting tumour angiogenesis is a latent method for treating CRC(3–6).

Many studies have demonstrated that the tumour microenvironment, including cancer-associated fibroblasts (CAFs) and tumour-associated macrophages (TAMs), promotes tumour angiogenesis(7–9). The tumour microenvironment, which is also termed the tumour mesenchyme or tumour stroma, includes CAFs, TAMs, blood vessels and extracellular matrix and substantially influences the initiation, growth and dissemination of colorectal cancer(2). Signal transducer and activator of transcription 3 (STAT3) belongs to a family of transcription factors that regulate the expression of genes involved in the pathogenesis of many human malignancies(10, 11). It was also reported that the TME activates STAT3 signalling in human umbilical vein endothelial cells (12), and the tumour microenvironment may affect angiogenesis through the STAT3 signalling pathway. In summary, the STAT3 pathway in blood vessels may become a target for the treatment of angiogenesis.

Bufalin (BU), the major bioactive component isolated from toad venom, has been confirmed to be a potent antitumour drug through its effect on tumour cell apoptosis, metastasis and proliferation(13, 14). In addition, bufalin also inhibits angiogenesis, and it was reported that the anti-angiogenic effect of sorafenib was signally increased in combination with bufalin by targeting AKT/VEGF in HUVECs(15). Wu et al. showed that bufalin enhanced cytocidal effects by targeting the STAT3 pathway(16).

Previously, we performed numerous studies on bufalin in the treatment of colorectal cancer(13, 17, 18). Here, we found that bufalin could reverse the pro-angiogenic effects mediated by TME. In the present study, we used in vitro angiogenesis-related experiments and in vivo subcutaneous tumour models and liver metastasis models to demonstrate that bufalin can inhibit TME-mediated STAT3 activation in endothelial cells to reduce angiogenesis and identified a new mechanism of bufalin in the treatment of CRC.

Materials And Methods

Cell culture

Cell were cultured in a humidified incubator with an atmosphere of 5% CO_2 at 37°C under normal oxygen conditions. Human umbilical vein endothelial cells (HUVECs, #8000, Sciencell, USA) were grown in endothelial cell medium (ECM, # 1001, Sciencell, USA) and only early passages (< p6) were used. CT26 cells were obtained from the Cell Bank of the Chinese Academy of Science s and were cultured in RPMI-1640 containing 10% FBS and 1% penicillin/streptomycin. The STAT3 overexpression plasmid were purchased from GeneChem (Shanghai, CN).

Conditioned medium (CM) preparation

CT26 cells and CAF were confirmed by morphological observation (Fig. S1a) and WB (Fig. S1b). The tumor cell supernatant polarizes the M0 macrophages, which was confirmed by morphological

observation and flow cytometry (Fig. S1c-d). After tumour-associated macrophages, cancer-associated fibroblasts, CT26 cells have grown to 80% of the bottom area of the flask, replace with FBS-free medium, at 48h post-treatment, cell suspensions were collected as conditioned medium. The CM was collected after high speed centrifugation and then pass 0.22 μm microporous mebrance, stored at -20˚C. In the same way, the cells were treated with 10 nM of bufalin for 24 hours, and then treated as above to obtain the relevant conditioned medium after drug action.

Tube formation assay.

HUVEC cells were incubated with conditioned medium for 24 hours before tube formation. Matrigel (BD, #356234, USA) was thawed overnight at 4˚C a day in advance, 50 μl of Matrigel was spread in a 96-well plate and polymerized at 37˚C for 30 minutes. Next, 3×10^4 HUVECs in 50 μl ECM were seeded to each well and incubated at 37°C in 5% CO_2 for 4 hours, photographed under the microscope.

Cell migration assay

HUVEC cells were incubated with conditioned medium for 24 hours before migration assay. 3×10^4 HUVECs in 300 μl of serum-free ECM mentioned earlier in the upper chamber and were seeded into a transwell insert (8.0 μm pore size, #353097, FALCON, USA), and allowed to migrate towards 700 μl of complete ECM. The non-migrated cells were removed from the upper part of the transwell with a cotton swab after 6 hours of incubation, and the insert was fixed with 4% paraformaldehyde for 10 minutes at room temperature. Transwell inserts were stained in 500 μl of 0.03% crystal violet solution for 30 minutes at 37℃.Then the insert was immersed and washed three times with PBS solution for 5 minutes each time, dried and photographed under the microscope.

Adhesion assay

After HUVEC cells were overgrown in a 24-well plate, they were treated with conditioned medium for 24 hours. Then 2×10^4 HCT116-GFP cells in 300 μl of serum-free ECM were inoculated on the treated HUVEC cells, and then incubated in a 37℃ incubator for 2 hours, washed with PBS three times, and then photographed under a fluorescence microscope.

Quantitative PCR

Total RNA was extracted from HUVEC using TRIzol (Invitrogen). The concentration of total RNA was quantified by measuring the absorbance at 260 nm. For SYBR Green-based quantitative PCR amplification, the reaction were carried out in a 20 μl reaction volume (Applied Biosystems). Using $2^{-\Delta\Delta Ct}$ method to determine the relative expression level of each cell line in each group.

The primer sequences were as follows: VEGF, 5’-TTGCTGCTCTACCTCCAC-3’ and 5’-AATGCTTTCTCCGCTCTG-3’; PDGFA, 5’-AGGCGTCCAGGCAGGTGATC-3’ and 5’-GCTTCTTCCTCGGTGCGTTCC-3’; E-selectin, 5’-ATGTTCAAGCCTGGCAGTTCCG-3’ and 5’-

GCAGAGCCATTGAGCGTCCATC-3’; P-selectin, 5’-CGCTCTGGACCAACCCTGTTTC-3’ and 5’-CTCCTGGCTTCTGTGGCTTGTG-3’.

Western Blot (WB)

The proteins separated by SDS-PAGE and subjected to immunoblotting to analyze antibodies (Abcam, USA). Blocked and incubated overnight at 4°C with primary antibodies. The membrane was further probed with horseradish peroxidase-conjugated anti-rabbit/mouse IgG antibody (Cell Signaling Technology, 1:5,000). Using ImageJ software to quantify protein bands.

In Vivo Xenograft Model

To determine the in vivo antiangiogenic activity of bufalin treatment, CT26-LUC cells (2×10^6) were injected into the flanks or spleen of male Balb/c mice (6 weeks old). One weeks after injection, bufalin (1 mg/kg) was administered by intraperitoneal (i.p.) injection once every other day for 21 days (flank) or 14 days (spleen). Subcutaneous tumour size was measured every three days and live imaging once a week after the treatment. The estimated tumor volumes (Vs) were calculated by the formula $V=W^2 \times L\times 0.5$, where W represents the largest tumor diameter in centimeters and L represents the next largest tumor diameter. Tumor-bearing mice were sacrificed after 21 or 14 days of treatment, and tumour tissues, spleen and liver were harvested, weighed, and then immediately fixed in formalin for follow-up experiment.

All experiments conformed to the ethical principles of animal experimentation stipulated by institutional animal care and use committee of Putuo Hospital, Shanghai University of Traditional Chinese Medicine, China.

Histopathological assay

The tissues were harvested after animals were sacrificed. The procedure of histopathological assay was accomplished by conventional hematoxylin-eosin (H&E) staining in accordance with standard techniques.

Immunofluorescence

2×10^4 HUVECs were seeded and cultured overnight on microscope coverslips (Thermo Fisher Scientific, Waltham, MA, USA). After treated with CM with or without bufalin for 24 hours as described previously, the cells were washed with PBS twice and fixed in methanol for 15 minutes, then permeabilized with 0.2% Triton X-100 (Beyotime, Shanghai, China) /PBS for 5 minutes and blocked by 3% BSA for 1 hours at room temperature. The coverslips were incubated with primary antibodies at 4°C overnight, and then incubated with secondary antibodies for 2 hours at 37°C (protected from light). Nuclear localization was assessed with 4',6-diamidino-2-phenylindole (DAPI, Beyotime, Shanghai, China).

Tissue sections were permeabilized with cold methanol for 5 minutes and incubated with 5% BSA in PBS for 1h. Primary antibodies were applied in blocking buffer and incubated overnight at 4°C. Dye-conjugated secondary antibodies were added in blocking buffer and incubated for 2 hours. Nuclei were stained with 4',6-diamidino-2-phenylindole (DAPI, Beyotime, Shanghai, China). Images were taken using Zeiss LSM880 confocal microscopy at the same voltage level and analyzed using ZEN Software.

Immunohistochemistry (IHC)

The tissue was fixed in 10% formalin, embedded in paraffin, and then sectioned (5 mm thick). The IHC of CD31 was performed as follows. The slides were dewaxed and incubated with 3% H_2O_2 aqueous solution for 10 minutes to quench the endogenous peroxidase activity. The heat-induced antigen recovery method was used to detect the antigen. Incubate the tissue with 5% BSA for 30 minutes at room temperature, and then incubate with the primary antibody in PBS at 4°C overnight. Using the appropriate secondary antibody to apply the indirect avidin-biotin-peroxidase method at room temperature for 30 minutes. EnVision (K4007, Dako) signal enhancement system was used to develop bound antibodies. The sections were stained with Harris hematoxylin, dehydrated and fixed. For quantification, 30 random images (400×) were captured with a microscope (Leica, Wetzlar, Germany) under each microscope.

Elisa

VEGF in HUVEC cells culture supernatants was evaluated by Human VEGF Quantikine ELISA Kit (R&D, Minnesota, USA) according to the manufacturer's protocol. VEGF in serum was evaluated by Mouse VEGF Quantikine ELISA Kit (R&D, Minnesota, USA) according to the manufacturer's protocol.

Statistical Analysis

Each experimental value is expressed as the mean ± SD. Statistical analysis was performed using t-test to evaluate the significance of the difference between the different groups, and the significance was accepted at *$p<0.05$, **$p<0.01$ and ***$p<0.001$. All data points represent the average of three repeated measurements. Spearman rank statistical test and Mann-Whitney test were used for statistical analysis of tissue samples to assess the significance of differences between groups.

Results

Bufalin suppresses angiogenesis induced by tumour microenvironment cells

Angiogenesis programming in tumour tissue is a multi-dimensional process, which is jointly regulated by cancer cells and various tumour-associated stromal cells and their biologically active products(7). CAFs, TAMs, and tumour cells are important components of the TME and contribute to tumour growth, metastasis, and neovascularization. Bufalin, as an active compound (Fig. 1a), has been reported to inhibit migration and invasion of hepatoma cells and lung cancer cell lines by down-regulating VEGF, which plays an important primary in tumour angiogenesis(19).

To clarify the effect of bufalin on angiogenesis caused by TME cells, we collected the supernatant of CT26 cells, CAFs and TAM as TME-conditioned media (CMs). Furthermore, we selected a low concentration IC_{15} (10 nM) and short treatment time (24 hours) by measuring the IC_{50} (30 nM) value of bufalin for HUVECs for 24 hours (Fig. 1b), to examine whether bufalin inhibits angiogenesis under these conditions to explore the mechanism by which bufalin affects the occurrence and development of colorectal cancer. The cell proliferation experiment showed that TME have no significant effect on HUVECs proliferation after treated by TME-CMs (CT26-CM, CAF-CM and TAM-CM) for 24 hours (Fig. 1c). The effect of bufalin on TME-mediated angiogenesis were determined by HUVEC tube formation, migration and adhesion experiments, and the results showed that bufalin inhibit angiogenesis induced by TME (Fig. 1d-f).

Bufalin suppresses TME-mediated angiogenesis by inhibiting angiogenic factors

To determine the mechanism of bufalin inhibit TME-mediated angiogenesis, we observed the expression of the angiogenesis-related and migratory factors VEGF and PDGFA and the vascular adhesion genes E-selectin and P-selectin in HUVECs treated with or without bufalin in combination with TME-CMs by quantitative PCR. The results showed that bufalin could significantly down-regulate those gene expression in HUVECs increased by TME (Fig. 2a-c).

Previous studies have shown that the STAT3 signaling pathway play a critical role in angiogenesis by inducing angiogenic factor, like VEGFs, PDGFs and so on(20, 21). In our study, the WB experiment showed bufalin could directly decease STAT3 phosphorylation in HUVECs activated by TME (Fig. 2d-f), and the results of immunofluorescence experiment also confirmed these findings (Fig. 2g). In addition, we found bufalin could inhibit VEGF expression by WB (Fig. 2d-f) and ELISA (Fig. 2h-j). Taken together, these results suggest that bufalin could inhibit STAT3 phosphorylation to decreased angiogenic factor expression induced by TME in vascular endothelial cells.

Bufalin suppresses TME-mediated angiogenesis by the STAT3 signaling pathway

To investigate whether the STAT3 signaling pathway is a key factor by which bufalin inhibits TME-mediated angiogenesis, we constructed a STAT3-overexpression (STAT3-OE) plasmid. STAT3 expression was confirmed by WB (Fig. S2a) and qPCR (Fig. S2b). We found that the STAT3-OE plasmid prevented bufalin-mediated inhibition of HUVEC tube formation (Fig. 3a), migration (Fig. 3b) and adhesion (Fig. 3c) induced by TME. These results suggest that bufalin inhibits TME-induced angiogenesis by the STAT3 signaling pathway, and STAT3 plays an important role in this process.

Bufalin suppresses TME-mediated angiogenesis by directly affecting vascular endothelial cells but not altering tumour microenvironment cells

Next, we determined whether bufalin also indirectly affects endothelial cells by changing TME cells. We first treated TME-cells (CT26, CAF & TAM) with 10 nM bufalin for 24 hours, replaced the medium with serum-free medium and collected the cell supernatant after an additional 24 hours for use as (TME+BU)-

CM, which was then used to treat HUVECs for 24 hours. Then, HUVEC tube formation (Fig. 4a), migration (Fig. 4b) and adhesion (Fig. 4c) were analysed. The results showed that bufalin did not affect vascular endothelial cells by affecting TME cells, and as the same as well, the WB results also proved that there are no significant differences in the increase in phosphorylated STAT3 levels in HUVECs induced by (TME+BU)-CMs and TME-CMs (Fig. 4d-f). Taken together, these results suggest that bufalin suppresses TME-mediated angiogenesis by directly affecting vascular endothelial cells but not altering TME-cells.

Bufalin inhibits CRC cells growth via anti-angiogenesis *in vivo*

To determine the effect of bufalin in vivo, a CRC cells xenograft model was established by using CT26 cells expressing luciferase (CT26-LUC). The schedule and scheme are shown in (Fig. 5a). All mice started treatment one week after xenotransplantation. The vehicle group was treated with normal saline, and the treatment group was administered bufalin (1 mg/kg). The volumes of the subcutaneous tumours (Fig. 5b) and in vivo imaging (Fig. 5c, Fig. S3b) were recorded during the treatment cycle (three weeks). Twenty-eight days after inoculation, the mice were sacrificed, subcutaneous tumours in the two groups of mice were weighted and photographed after the treatment was over (Fig. 5d). The results showed that bufalin significantly inhibited the growth of tumours compared with the vehicle without affecting animal body weights (Fig. S3a), which proved that bufalin had no serious toxic effects on the body. To further confirm the anti-angiogenesis effect obtained in vitro, we conducted IHC to evaluate the expression of CD31 and Ki67 in tumours, the results of IHC showed the reduction of proliferation and subcutaneous tumor blood vessels in the bufalin group (Fig. 5e). Next, we measured the serum VEGF levels in the two groups of mice by ELISA, and the results showed that the serum VEGF levels in the bufalin group were significantly lower than those in the vehicle group (Fig. 5f). Moreover, we also examined the activation of vascular p-STAT3 in solid tumours. The immunofluorescence results showed that the number of blood vessels in subcutaneous tumours and the proportion of activated p-STAT3-positive blood vessels in the bufalin group were significantly lower than those in the vehicle group (Fig. 5g). These data indicated that bufalin inhibits angiogenesis by targeting the activation of p-STAT3 in tumour blood vessels, thereby inhibiting tumour growth in a CRC cells xenograft model.

Bufalin inhibits CRC cells metastasis via anti-angiogenesis *in vivo*

Cancer metastasis remains a major challenge to the successful management of malignant diseases. The liver is the main site of metastatic disease and a major cause of death from colorectal cancer(22). To investigate the effect on bufalin inhibiting CRC cells metastasis via anti-angiogenesis in vivo, we established a CRC cells liver metastasis model (Fig. 6a), and tumour metastasis was observed by an in vivo imaging system from day 7 to day 21 (Fig. 6b, Fig. S4b). The in vivo imaging results showed that after one week of bufalin treatment, bufalin began to inhibit liver metastasis compared to that of the vehicle group, and until the mice were sacrificed on day 21, bufalin significantly inhibited liver metastasis by more than 50% compared to that of the vehicle without affecting animal body weights (Fig. S4a). Metastatic foci of considerable sizes were visible in the livers of mice treated with vehicle. Haematoxylin-eosin–stained liver sections were examined under a microscope, and as expected, the formation of

metastases in the liver was reduced by approximately 80% by bufalin treatment (Fig. 6c-d). The results of IHC showed the reduction of blood vessels in spleen and liver metastases in the bufalin group (Fig. 6e). Similarly, mice treated with bufalin had a significantly lower serum VEGF levels than mice treated with the vehicle (Fig. 6f). Consistent with the subcutaneous tumours, the immunofluorescence results showed that the number of blood vessels in liver tumours and p-STAT3-positive blood vessels significantly decreased after bufalin treatment (Fig. 6g). Interestingly, p-STAT3 in endothelial cells was only activated in the tumour site, while it was rarely activated in normal liver tissues. This result further suggests that bufalin inhibits liver metastasis by targeting STAT3 in tumour blood vessels not only in primary tumours but also in metastatic tumours.

Discussion

Accumulating evidence has substantiated that angiogenesis plays a critical role in tumour progression and that inhibiting angiogenesis is a promising strategy for tumour treatment. Angiogenic programming in neoplastic tissue is a multidimensional process regulated by tumour cells in conjunction with various tumour-associated stromal cells, as well as the TME(9, 23–25). We found that bufalin could reverse angiogenesis mediated by the TME.

Anti-angiogenesis therapy is an important strategy for the treatment of CRC. Previous studies have reported that bufalin can synergistically enhance the anti-angiogenic effect of sorafenib via AKT/VEGF signalling(15). We found that bufalin could inhibit the tube formation, adhesion and migration of HUVECs mediated by CAFs, TAMs and tumour cells by inhibiting the activation of HUVEC STAT3 and thereby decreasing the expression of VEGF, PDGFA, E-selectin, and P-selectin. Similarly, we established subcutaneous tumour models and liver metastasis models in vivo and found that bufalin inhibited the growth and metastasis of CRC by significantly reducing the number of blood vessels and STAT3 phosphorylation in vascular endothelial cells. In addition, the serum concentration of VEGF after bufalin treatment was also significantly reduced. This finding indicated that bufalin targets the STAT3 signalling pathway to reduce TME-mediated angiogenesis.

STAT3 is a transcription factor that regulates various kinds of cellular events, including differentiation, apoptosis and proliferation. Previous studies have shown that STAT3 activation promotes tumour angiogenesis by increasing VEGF expression(26, 27). Intercellular communication between the TME and vascular endothelial cells is promoted by STAT3(28). Notably, STAT3 is one of the important targets of bufalin, and bufalin can inhibit STAT3 activity. Moreover, we found that STAT3 overexpression could reverse the inhibitory effect of bufalin on angiogenesis. Collectively, we propose a model in which bufalin reduces the expression of angiogenesis genes by inhibiting the phosphorylation of STAT3 on endothelial cells, thereby antagonizing the pro-angiogenic effect of the tumor microenvironment (Fig. 7)

More interestingly, we found that bufalin could suppress TME-mediated angiogenesis. Furthermore, we treated CAFs, TMAs and tumour cells with bufalin and then used the conditioned cell supernatant to treat HUVECs and found no promotion of tube formation, migration or adhesion. Notably, compared to some

previous antitumour studies of bufalin(29, 30), we chose a lower bufalin concentration and a shorter treatment time for both in vitro and in vivo experiments, which ruled out the direct effect of bufalin on TME cells. These results suggest a new mechanism by which low concentrations of bufalin affect TME-mediated angiogenesis by directly acting on the STAT3 signalling pathway on vascular endothelial cells but not on TME cells, and this effect is characterized by low toxicity and high efficiency.

In summary, our results show that the TME promotes tumour angiogenesis by activating STAT3 in vascular endothelial cells and that bufalin can precisely inhibit angiogenesis by targeting STAT3. Through our research, we have enriched the understanding of the antitumour effect of bufalin, which can indirectly inhibit TME-mediated angiogenesis. In the future, bufalin may be developed as a new type of anti-angiogenic auxiliary drug.

Conclusions

In summary, bufalin suppresses tumour microenvironment-mediated angiogenesis by inhibiting the STAT3 signaling pathway. Tumor microenvironment promotes tumour angiogenesis by activating STAT3 in vascular endothelial cells, and that bufalin can precisely inhibit angiogenesis by targeting STAT3 which reveals that bufalin may be used as a new anti-angiogenic adjuvant therapy medicine in the treatment of colorectal cancer.

Abbreviations

STAT3: Signal transducer and activator of transcription 3; TME: Tumor microenvironment; HUVEC: Human umbilical vein endothelial cells; CRC: Colorectal cancer; CAF: Cancer-associated fibroblast; TAM: Tumour-associated macrophage; BU: Bufalin; CM: Conditioned medium; WB: Western Blot; PCR: Polymerase chain reaction; IHC: Immunohistochemistry; Elisa: Enzyme linked immunosorbent assay.

Declarations

Acknowledgements

Not applicable.

Authors’s contributions

K.X., X.L., and P.Y. conceived and directed the project. K.X. designed the experiments. K.F., Y.W., C.W., R.Z., and M.S. carried out the experiments. K.X., K.F., and Y.Z. conducted the data analysis and interpreted the results. K.F., K.X., Y.Z., X.L., and P.Y. wrote and edited the paper. All authors read and approved the final manuscript.

Funding

This project was sponsored by the Science and technology innovation project of Putuo District Health system (ptkwws201905), the Budget project of Shanghai University of Traditional Chinese Medicine (2019LK039) and the Natural Science Foundation of Shanghai (20ZR1450500,19ZR1413800). This project was also sponsored by the National Nature Science Foundation of China (81873137).

Availability of data and materials

The datasets during and/or analysed during the current study available from the corresponding author on reasonable request.

Ethics approval and consent to participate

Not applicable.

Consent for publication

Not applicable.

Competing interests

The authors declare that they have no conflict of interest.

References

1. Bray F, Ferlay J, Soerjomataram I, et al. Global cancer statistics 2018: GLOBOCAN estimates of incidence and mortality worldwide for 36 cancers in 185 countries. CA Cancer J Clin. 2018;68(6):394–424.
2. Kobayashi H, Enomoto A, Woods SL, et al. Cancer-associated fibroblasts in gastrointestinal cancer. Nat Rev Gastroenterol Hepatol. 2019;16(5):282–95.
3. Battaglin F, Puccini A, Intini R, et al. The role of tumor angiogenesis as a therapeutic target in colorectal cancer. Expert Rev Anticancer Ther. 2018;18(3):251–66.
4. Mesange P, Bouygues A, Ferrand N, et al. Combinations of Bevacizumab and Erlotinib Show Activity in Colorectal Cancer Independent of RAS Status. Clin. Cancer Res. 2018;24(11):2548–58.
5. Tournigand C, Chibaudel B, Samson B, et al. Bevacizumab with or without erlotinib as maintenance therapy in patients with metastatic colorectal cancer (GERCOR DREAM; OPTIMOX3): a randomised, open-label, phase 3 trial. Lancet Oncol. 2015;16(15):1493–505.
6. Ranieri G, Patruno R, Ruggieri E, et al. Vascular endothelial growth factor (VEGF) as a target of bevacizumab in cancer: from the biology to the clinic. Curr Med Chem. 2006;13(16):1845–57.
7. Palma MD, Biziato D, Petrova TV. Microenvironmental regulation of tumour angiogenesis. Nat Rev Cancer. 2017;17(8):457–74.
8. Jiang X, Wang J, Deng X, et al. The role of microenvironment in tumor angiogenesis. J Exp Clin Cancer Res. 2020;39(1):75.

9. Unterleuthner D, Neuhold P, Schwarz K, et al. Cancer-associated fibroblast-derived WNT2 increases tumor angiogenesis in colon cancer. Angiogenesis. 2019;23(2):159–77.
10. Don-Doncow N, Marginean F, Coleman I, et al. Expression of STAT3 in Prostate Cancer Metastases. Eur Urol. 2017;71(3):313–6.
11. Pan Y-M, Wang C-G, Zhu M, et al. STAT3 signaling drives EZH2 transcriptional activation and mediates poor prognosis in gastric cancer. Mol Cancer. 2016;15(1):79.
12. Du Y-e, Tu G, Yang G, et al. MiR-205/YAP1 in Activated Fibroblasts of Breast Tumor Promotes VEGF-independent Angiogenesis through STAT3 Signaling. Theranostics. 2017;7(16):3972–88.
13. Zhan Y, Qiu Y, Wang H, et al. Bufalin reverses multidrug resistance by regulating stemness through the CD133/nuclear factor-κB/MDR1 pathway in colorectal cancer. Cancer Sci. 2020;111(5):1619–30.
14. Huang WW, Yang JS, Pai SJ, et al. Bufalin induces G 0/G 1 phase arrest through inhibiting the levels of cyclin D, cyclin E, CDK2 and CDK4, and triggers apoptosis via mitochondrial signaling pathway in T24 human bladder cancer cells. Mutation Research - Fundamental Molecular Mechanisms of Mutagenesis. 2012;732(1–2):26–33.
15. Wang H, Zhang C, Ning Z, et al. Bufalin enhances anti-angiogenic effect of sorafenib via AKT/VEGF signaling. Int J Oncol. 2016;48(3):1229–41.
16. Wu X, Tian F, Su M, et al. BF211, a derivative of bufalin, enhances the cytocidal effects in multiple myeloma cells by inhibiting the IL-6/JAK2/STAT3 pathway. Int Immunopharmacol. 2018;64:24–32.
17. Sun J, Xu K, Qiu Y, et al. Bufalin reverses acquired drug resistance by inhibiting stemness in colorectal cancer cells. Oncol Rep. 2017;38(3):1420–30.
18. Yin P, Wang Y, Qiu Y, et al. Bufalin-loaded mPEG-PLGA-PLL-cRGD nanoparticles: preparation, cellular uptake, tissue distribution, and anticancer activity. Int J Nanomedicine. 2012;7:3961–9.
19. Jiang Y, Zhang Y, Luan J, et al. Effects of bufalin on the proliferation of human lung cancer cells and its molecular mechanisms of action. Cytotechnology. 2010;62(6):573–83.
20. Liu J, Deng W, Chen L, et al. Inhibition of JAK2/STAT3 reduces tumor-induced angiogenesis and myeloid-derived suppressor cells in head and neck cancer. Mol Carcinog. 2018;57(3):429–39.
21. Liang L, Hui K, Hu C, et al. Autophagy inhibition potentiates the anti-angiogenic property of multikinase inhibitor anlotinib through JAK2/STAT3/VEGFA signaling in non-small cell lung cancer cells. J Exp Clin Cancer Res. 2019;38(1):71.
22. Brodt P. Role of the Microenvironment in Liver Metastasis: From Pre- to Prometastatic Niches. Clin Cancer Res. 2016;22(24):5971–82.
23. Jetten N, Verbruggen S, Gijbels M, et al. Anti-inflammatory M2, but not pro-inflammatory M1 macrophages promote angiogenesis in vivo. Angiogenesis. 2014;17(1):109–18.
24. Britto D, Wyroba B, Chen W, et al. Macrophages enhance Vegfa-driven angiogenesis in an embryonic zebrafish tumour xenograft model. Dis Model Mech. 2018;11(12):dmm035998.
25. Zhang T, Liu L, Lai W, et al. Interaction with tumorassociated macrophages promotes PRL3induced invasion of colorectal cancer cells via MAPK pathwayinduced EMT and NFkappaB signalinginduced

angiogenesis. Oncol Rep. 2019;41(5):2790–802.
26. Wei D, Le X, Zheng L, et al. Stat3 activation regulates the expression of vascular endothelial growth factor and human pancreatic cancer angiogenesis and metastasis. Oncogene. 2003;22(3):319–29.
27. Niu G, Wright KL, Huang M, et al. Constitutive Stat3 activity up-regulates VEGF expression and tumour angiogenesis. Oncogene. 2002;21(13):2000–8.
28. Kujawski M, Kortylewski M, Lee H, et al. Stat3 mediates myeloid cell-dependent tumor angiogenesis in mice. J Clin Invest. 2008;118(10):3367–77.
29. Zhang Y, Dong Y, Melkus M, et al. Role of P53-Senescence Induction in Suppression of LNCaP Prostate Cancer Growth by Cardiotonic Compound Bufalin. Mol Cancer Ther. 2018;17(11):2341–52.
30. Liu X, Zhou Y, Peng J, et al. Silencing c-Myc Enhances the Antitumor Activity of Bufalin by Suppressing the HIF-1alpha/SDF-1/CXCR4 Pathway in Pancreatic Cancer Cells. Front Pharmacol. 2020;11:495.

Figures

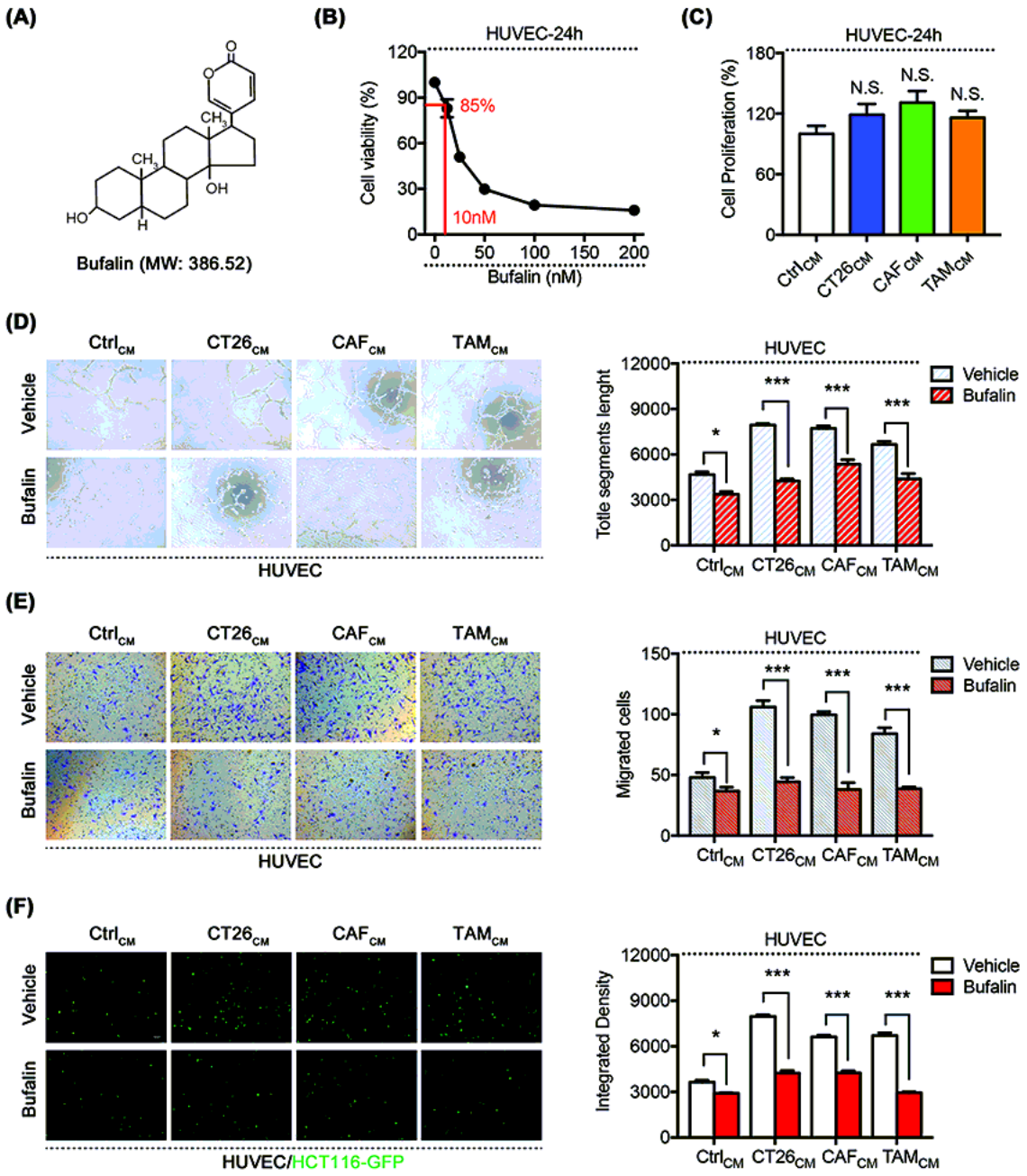

Figure 1

Bufalin suppresses angiogenesis induced by tumour microenvironment cells. a Molecular structure of BU. b Cell viability of HUVEC after treated with BU for 24h. c Cell proliferation of HUVEC after treated with different TME-CMs for 24h. The effect of bufalin (BU) on the tube formation (d), migration (e) and adhesion (f) of HUVECs in response to different TME-CMs. *P<0.05, **P<0.01, ***P<0.001. Each bar represents the mean ± SD of three independent experiments. BU, bufalin

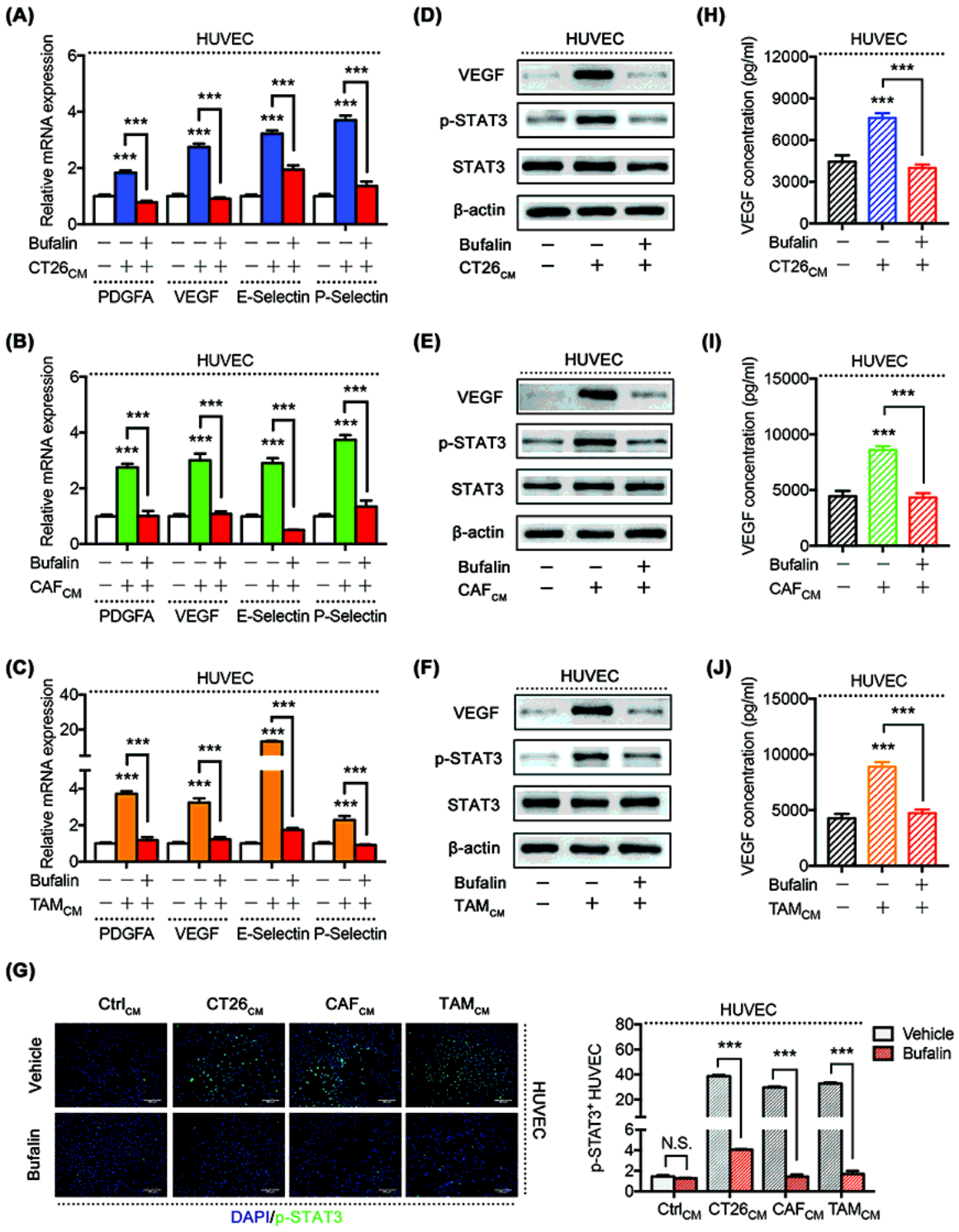

Figure 2

Bufalin suppresses TME-mediated angiogenesis by inhibiting angiogenic factors. Relative PDGFA, VEGF, E-selectin and P-selectin mRNA expression in HUVECs after treatment with CT26-CM (a), CAF-CM (b) or TMA-CM (c) with or without bufalin (BU). d-f WB showing the protein expression of VEGF, p-STAT3 and STAT3 in HUVECs treated with different TME-CMs in the presence or absence of BU, membranes were stripped and re-probed with total β-actin as a control. g-i The concentration of VEGFA in HUVEC

supernatant after treatment with different TME-CMs in the presence or absence of BU. j Immunofluorescence analysis showing p-STAT3+ HUVECs after treatment with different TME-CMs in the presence or absence of BU. *P<0.05, **P<0.01, ***P<0.001. Each bar represents the mean ± SD of three independent experiments. BU, bufalin

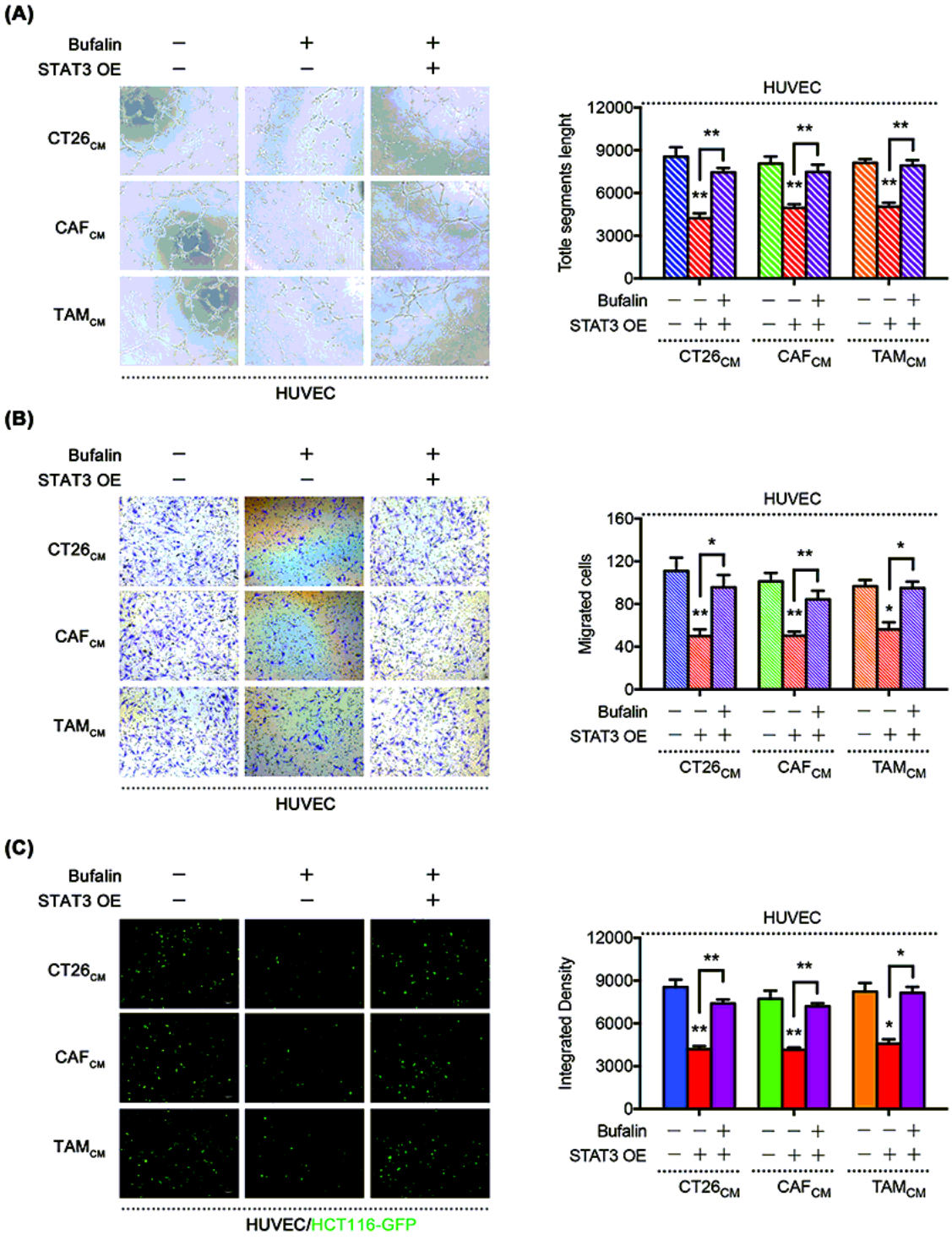

Figure 3

Bufalin suppresses TME-mediated angiogenesis by the STAT3 signaling pathway. Tube formation (a), migration (b) and adhesion (c) of HUVECs after treatment with TME-CMs and BU with or without the STAT3-OE plasmid. *P<0.05, **P<0.01, ***P<0.001. Each bar represents the mean ± SD of three independent experiments. BU, bufalin

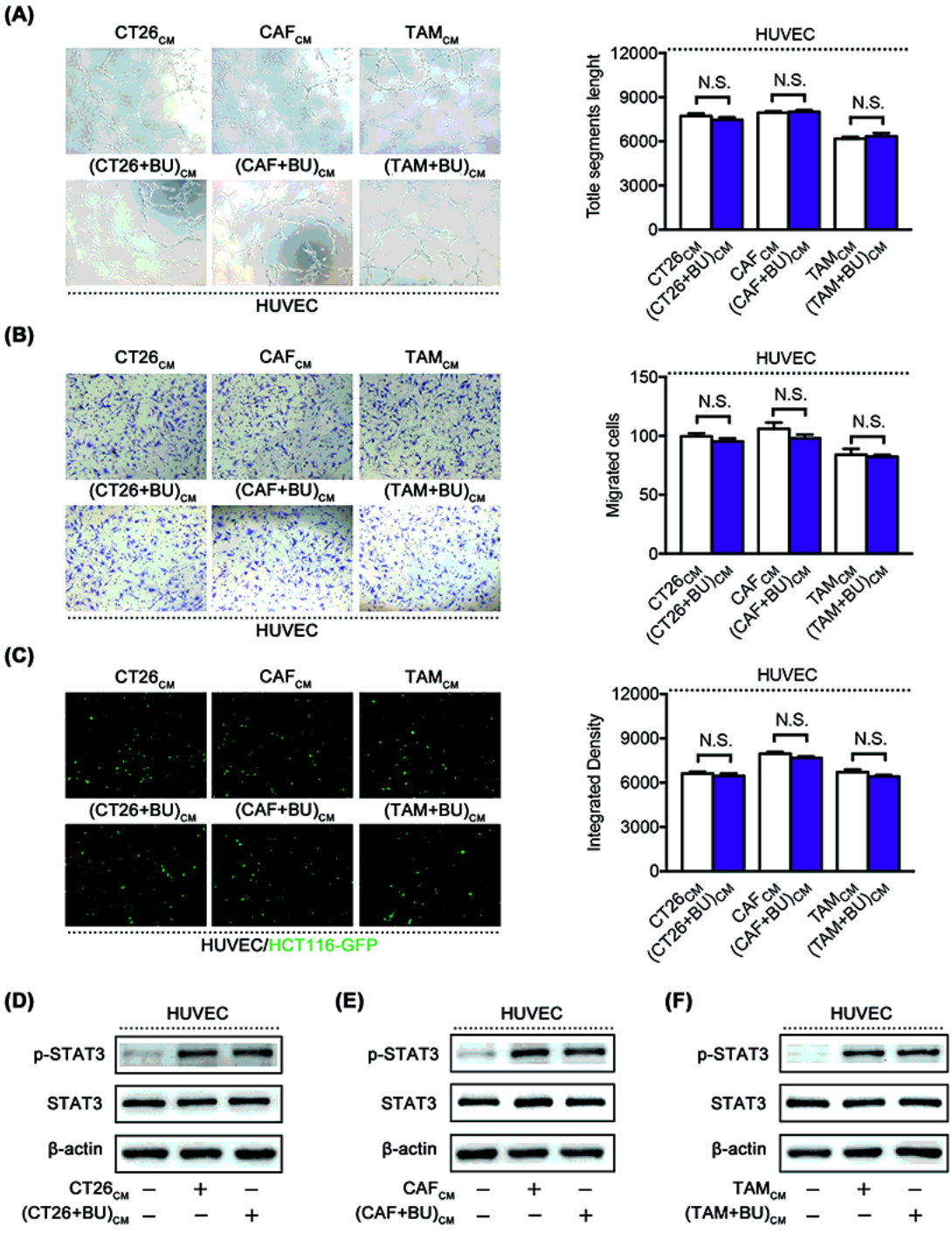

Figure 4

Bufalin suppresses TME-mediated angiogenesis by directly affecting vascular endothelial cells but not altering tumour microenvironment cells. Tube formation (a), migration (b), and adhesion (c) of HUVECs treated with TME-CMs and TME+BU-CMs for 24 hours. d-f WB showing the protein expression of p-STAT3 and STAT3 in HUVECs treated with different TME-CMs and TME+BU-CMs, membranes were stripped and re-probed with total β-actin as a control. N.S. indicates no significant difference between the two groups, P>0.05. BU, bufalin

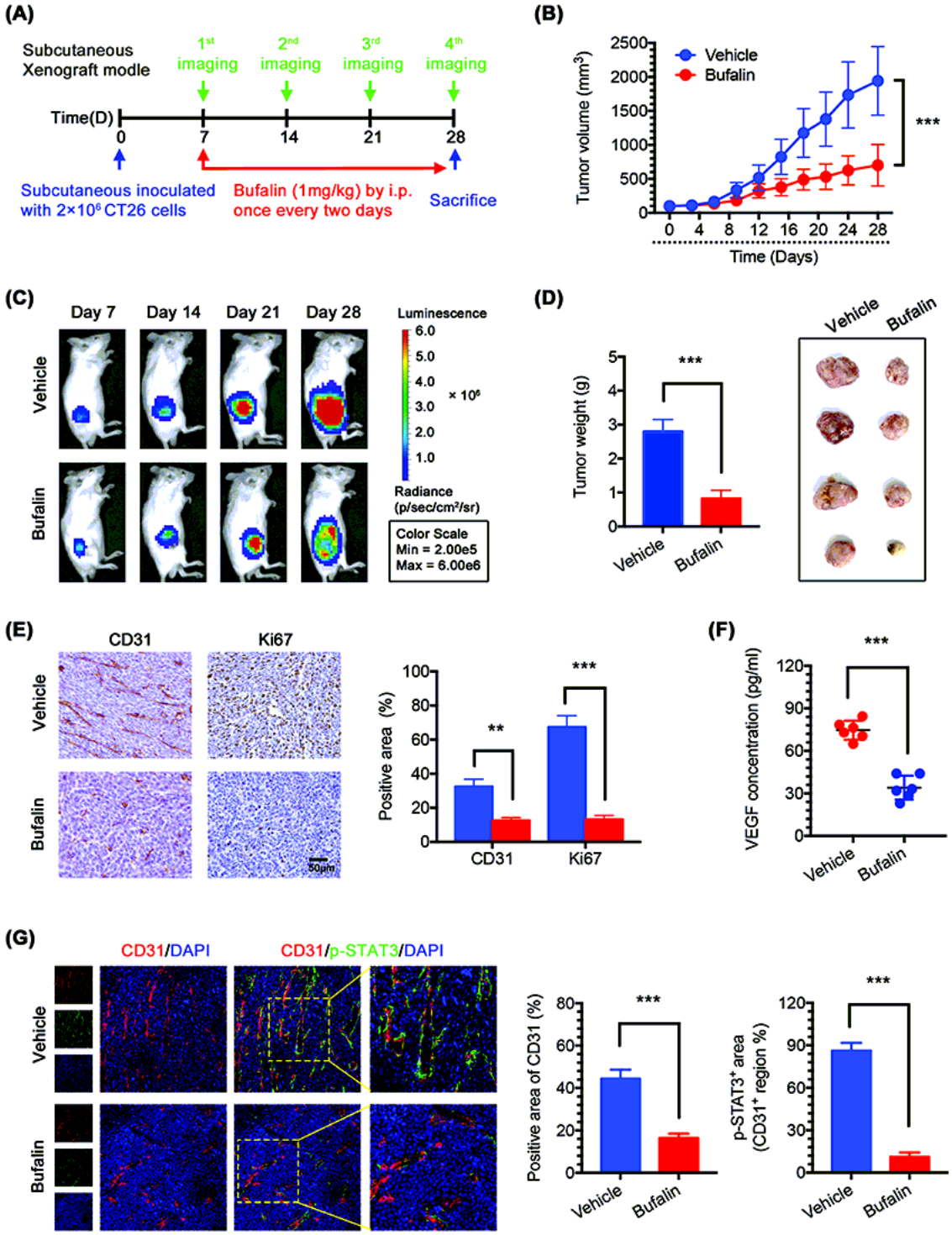

Figure 5

Bufalin inhibits CRC cells growth via anti-angiogenesis in vivo. a Scheme and schedule of imaging and treatments. b Tumour volumes from day 0 to day 28. c Tumour growth was visualized by an in vivo imaging system from day 7 to day 28. d Tumour weights and images. e IHC analysis of CD31 and Ki67 in tumours. f VEGF expression level in serum. g Immunofluorescence analysis of CD31 and p-STAT3 in tumours. **P<0.01, ***P<0.001. Each bar represents the mean ± SD of three independent experiments. IHC, immunohistochemistry

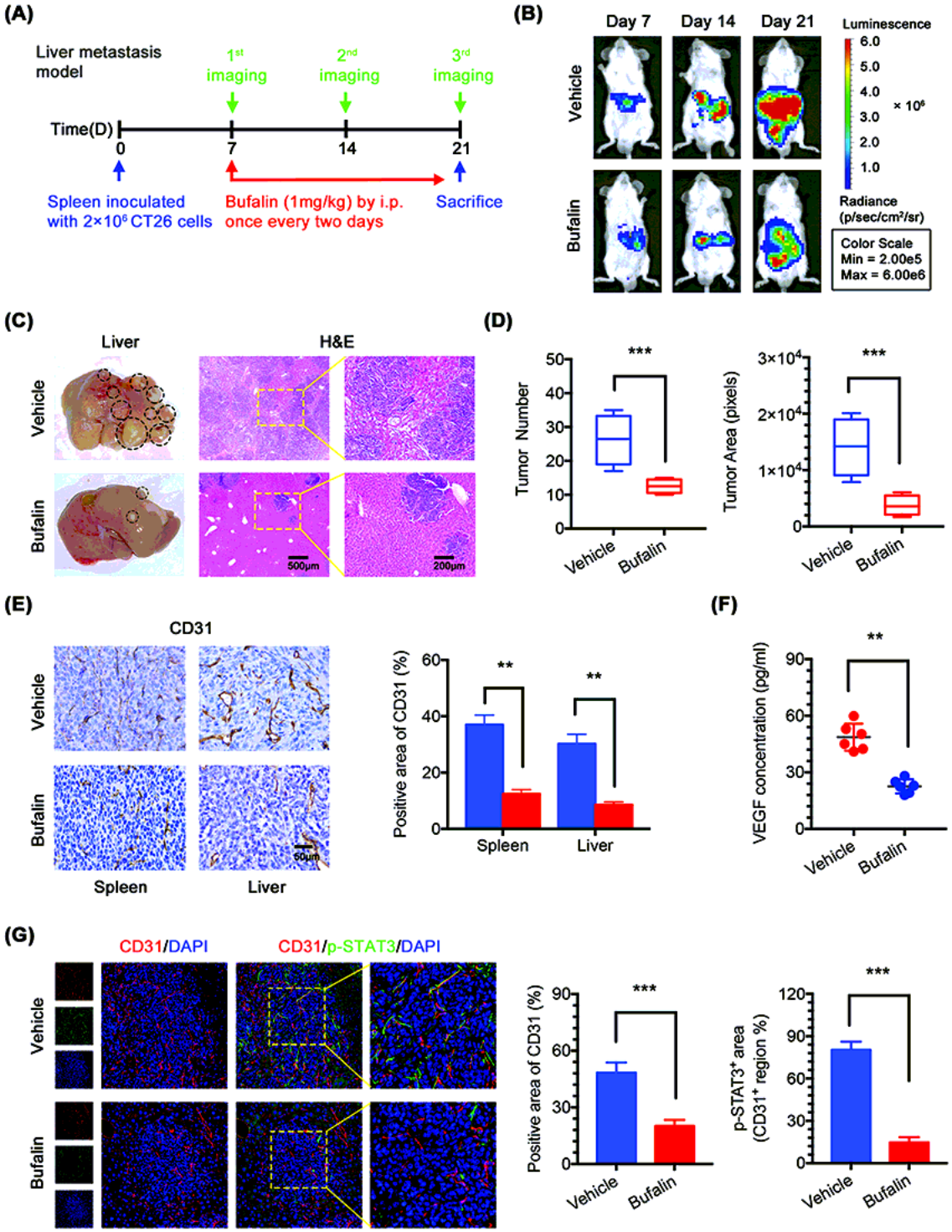

Figure 6

Bufalin inhibits CRC cells metastasis via anti-angiogenesis in vivo. a Scheme and schedule of imaging and treatments. b Tumour metastasis was visualized by an in vivo imaging system from day 7 to day 21. c Representative images of liver and H&E-stained liver tissue. d Tumour number and area in liver. e IHC analysis of CD31 in spleen and liver tissue. f VEGF expression level in serum. g Immunofluorescence analysis of CD31 and p-STAT3 in liver. **P<0.01, ***P<0.001. Each bar represents the mean ± SD of three independent experiments. IHC, immunohistochemistry

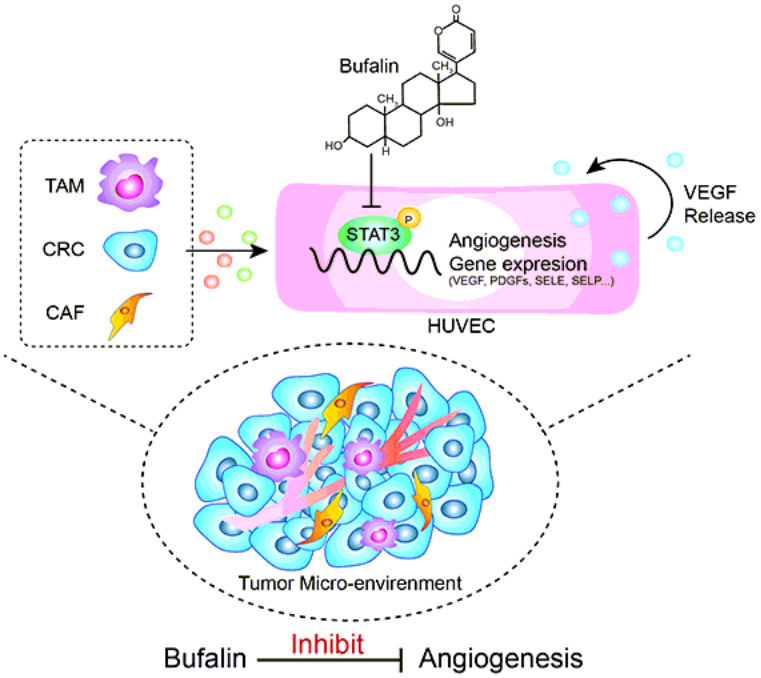

Figure 7

The mechanism of BU inhibiting tumor microenvironment-mediated angiogenesis.

Supplementary Files

This is a list of supplementary files associated with this preprint. Click to download.

- SFig1.tif
- SFig2.tif
- SFig3.tif
- SFig4.tif